

Investigation of gallium nitride T-ray transmission characteristics

Bradley Ferguson^{* a,b}, Samuel Mickan^{* a}, Seth Hubbard^c, Dimitris Pavlidis^{* c}
and Derek Abbott^{* a}

^a Centre for Biomedical Engineering and
Department of Electrical & Electronic Engineering,
Adelaide University, SA 5005, Australia

^b CRC for Sensor, Signal and Information Processing,
Technology Park, Mawson Lakes Boulevard, Mawson Lakes, SA 5095, Australia

^c Department of Electrical Engineering and Computer Science,
The University of Michigan, Ann Arbor, MI 41809, U.S.A.

ABSTRACT

T-ray imaging and spectroscopy both exploit the terahertz (THz) region of the spectrum. This gives rise to very promising industrial and biomedical applications, where non-invasive and sensitive identification of a substance is achievable, through a material's distinct absorption features in the THz band. Present T-ray systems are limited by low output power, and the race is now on to find more efficient THz emitters. We discuss the feasibility of a novel high-power gallium nitride emitter for terahertz generation. This paper details the advantages of such an emitter, primarily by virtue of its high-voltage capability, and evaluates the benefits of sapphire and silicon carbide substrates. The far-infrared transmission spectra for thin samples of GaN, sapphire and SiC are reported. A high-power THz emitter, that operates at room temperature and is potentially low-cost will open up a host of new possibilities and applications. The central result in this paper demonstrates that sapphire is the better choice over SiC, for the GaN supporting substrate, as we show that it has superior THz transmission characteristics.

Keywords: Terahertz, gallium nitride, T-rays, photoconductive antenna

1. INTRODUCTION

The T-ray or terahertz (THz) region of the spectrum lies on the border of electronics and optics. Microwaves are generated using high-speed oscillating devices, while infrared radiation is generated thermally or using other light sources. T-rays are situated between these two - and this 'borderline status' is one reason why this frequency has been difficult to access thus far. Infrared sources become very dim as we approach the THz region and to this day high-speed electronic devices struggle to radiate much above 500 GHz. However, recent advances in femtosecond laser technology have facilitated the convenient generation of short bursts of THz radiation, thus opening up a new part of the spectrum for further study. Shen et al¹⁻³ were the first to generate pulsed FIR using a technique known as optical rectification. In the late 1980's Columbia University improved the technique using superior phase matching and this allowed them to achieve a broader frequency response,⁴ however the technique remained the domain of a select few ultrafast laser laboratories until the mid-1990's when AT&T Bell Labs successfully demonstrated terahertz pulse imaging, coining the term 'T-rays.'

Until about 5-6 years ago, T-ray techniques involved femtosecond lasers pumped by cumbersome argon lasers occupying the length of a whole room with 3-phase power. Now small and compact high-power semiconductor-diode pump lasers are replacing the tabletop optics jungle, making simple turnkey solutions for portable T-ray

*Email: bradley.ferguson@ieee.org, spm@ieee.org, pavlidis@umich.edu, dabbott@eleceng.adelaide.edu.au;
Telephone: +61 8 8303 6296; Fax: +61 8 8303 4360

applications a foreseeable option, and are spurring many groups world-wide to research diverse new application ideas from biomedicine to semiconductor testing.

One of the crucial properties of terahertz radiation is that, at 1 THz, water has an absorption coefficient of 230/cm and hence is excellent for detecting low levels of moisture, as sensitively as 1 part in a million.⁵ As well as water, many polar liquids, for example solvents, and most gases have very strong absorption lines in the THz range.⁶ Also metal and semiconductor carriers have their largest response in this range, and the absorption and dispersion of dielectrics are dominated by the molecular vibrations of the materials.⁶ As both amplitude and phase are measured in T-ray detection, different substances can be identified from details of the distorted pulse shape after it has passed through the sample - this pulse shape can be used as the 'signature' of a particular substance as it depends on the exact frequency dependence of absorption and dispersion.⁶ T-ray time domain spectroscopy (TDS) is of critical importance in the spectroscopy of condensed matter systems, trace gas analysis and a number of other applications.⁵ In contrast, dry, non-metallic materials such as plastics, paper and cardboard are transparent to T-rays.⁶ This suggests the possibility that T-rays can be used in the quality control of food through a sealed non-metallic package or wrapper.

The extreme sensitivity of T-rays to water content is of great interest in the area of food technology, with obvious application in the area of quality control of food and packaging. Another important impact on the food industries, may be T-ray applications that benefit agricultural science. T-rays can be employed to non-destructively monitor the water flow dynamics within a living transpiring plant or crop.⁵ Such experiments can be used to further understand the early warning signs of plant water stress, and thus T-ray imaging has exciting application as an aid in irrigation management. Non-invasive sensitive moisture analysis is also of extreme interest to the plastics industry, for quality control.

T-ray imaging for medical applications is limited to the surface of the human body, for example for scrotal, corneal and dermatological/cutaneous imaging, but could find important use in estimating the depth of burns⁷ and early warning signs of skin cancer.⁸ The level of image differentiation at these shallow depths is more precise than with the use of X-rays. Unlike X-rays, T-rays have the advantage of being a non-ionising radiation and hence are not dangerous in terms of imparting cancer. Due to these significant advantages, cutaneous imaging for biomedical diagnostics is a significant application focus. We have made initial experiments demonstrating clearly distinct T-ray spectra between meat and fat in a sample of ham.⁹ Cambridge University has an ongoing T-ray program, jointly with Toshiba, focussed on detecting dental decay.¹⁰ The NIST in Washington DC have also recently been able to obtain T-ray spectra for DNA, bovine serum albumin and collagen.¹¹

A fundamental point, in support of the use of T-rays in biomedical applications, is the fact that Rayleigh scattering is inversely proportional to the fourth power of wavelength. At optical frequencies, scattering is significant in biological tissue, whereas at microwave frequencies Rayleigh scattering is insignificant, but the wavelength is large thus limiting resolution. T-rays represent the ideal trade-off between these two extremes.¹²

T-rays are by no means limited to food, agricultural and medical applications. There is great military interest in that the usual 0.5 to 10 GHz signature of boats/aircraft/tanks is identical to the scattered field from 1/200 scaled down models over the 100 GHz to 2 THz range. Hence T-ray detection can be used to simulate real military scenarios in the laboratory. DARPA have recently initiated a \$US 12 million program for inter-satellite communications in the THz band. Furthermore, a group at Berkeley have found that T-rays have just the right energy to break Cooper pairs in superconductors and are using this effect to further understand distortion mechanisms in superconducting microwave filters.¹³ Broadband THz reflectometry is also being investigated as a powerful diagnostic tool for high-temperature plasmas - it is the *coherent* detection of THz waveforms that permits the imaging of thermally active media, an ability not possessed by other far-infrared detection systems. In the field of quantum computation coherent THz beams are used in manipulate quantum bits (qubits) for decoherence experiments in semiconductor materials.¹⁴

T-ray imaging is based on optoelectronic terahertz time-domain spectroscopy (TDS). The idea of T-ray imaging is to combine spectroscopic measurements with real-time imaging and advanced signal processing, so that each pixel of the image contains spectroscopic information about the object. A typical T-ray imaging system usually consists of the following main elements: (a) a femtosecond optical pulse source (b) an optically gated emitter of THz transients with broad spectral bandwidth (c) an imaging system consisting of lenses

and/or mirrors (d) an object under investigation (e) a time-gated detector (f) a scanned mirror that introduces an optical path delay between the femtosecond gating pulses on the THz emitter and detector (g) a computer to process the time domain data (h) and a display to view the image.

A pump/probe configuration uses a scanned mirror to vary the optical path between the pump and probe pulses - this enables the extraction of phase as well as amplitude information. Thus both phase and amplitude spectra can be directly and accurately obtained without use of the Kramers-Kronig relation. After data acquisition of the THz waveforms on a computer, both with the object in place and the object removed (reference), a numerical FFT is typically performed to enable deconvolution of the unwanted system response and then to extract both amplitude and phase information.

2. T-RAY GENERATION

There are a number of possible methods for generating broadband terahertz radiation, however there are only two commonly used, efficient and practical techniques: (a) optical rectification and (b) photoconductive antennas. The first method has a theoretically wider bandwidth - in method (a), broadband T-rays are essentially generated by illuminating an electro-optic crystal with red femtosecond pulses. This exploits the χ^2 optical nonlinearity of GaAs, to produce difference frequencies of the original Fourier components. The photoconductive antenna was first demonstrated in the 1980's by Mourou^{15,16} in the GHz range and then shortly after by Auston⁴ at Columbia University in the THz range. This method promises higher THz beam power, but at the sacrifice of bandwidth. Method (a) theoretically can offer bandwidths over 30 THz, whereas, (b) presently goes up to around 4 THz - for the promise of increased beam power, this trade-off is tenable for biomedical applications given that the NIST were able to characterise bovine collagen, albumen and DNA in the 0.1 to 2 THz range.¹¹

Photoconductive antennas are produced by lithographically patterning two metal electrodes on the surface of a semiconductor substrate, such as a GaAs wafer. A bias is applied across the two electrodes and a high field region is generated in the material. A femtosecond laser is focussed in the gap between the two electrodes generating electron-hole pairs, these photogenerated carriers which are injected into the high field region end up accelerating and drifting in opposite directions depending on whether they are electron or hole charges. As a result of this transport, a space-charge field is generated which screens the bias field. As the light source is a femtosecond laser, a transient current is set up between the two electrodes in regular bursts, causing the electrodes to radiate as a dipole antenna.

The resulting THz output beam average power is proportional to the square of the electrode bias.¹⁷ So it would seem that increasing the power is a simple matter of increasing the bias. However, a GaAs substrate undergoes semiconductor breakdown with bias voltages greater than approximately 40 Volts, for an electrode spacing in the order of 1 μm . Hence our proposal, here, is to exploit the high-voltage breakdown characteristic of GaN and thereby investigate high-power THz emitters on GaN substrates. Due to the square dependence of power on bias, this approach is very promising. The breakdown field in GaAs is 400 kV/cm and in GaN it is 2000 kV/cm. This is a 5 fold increase in breakdown threshold, for a given electrode spacing, which corresponds to over a 25 fold (or 14 dB) increase in THz power on the square law basis.

3. INVESTIGATION OF GALLIUM NITRIDE

Presently conversion efficiencies in photoconductive antennas are low and consequently average THz beam powers tend to be in the nW to μW range - whereas the average power of the femtosecond optical source is in the region of 1 W. This illustrates the huge inefficiencies in present-day systems. The race is now on world-wide to perform research to increase the THz power. Approaches in the literature are either impractical, expensive or fraught with problems. For example, some groups report the use of an organic crystal called DAST¹⁸ that has a much greater conversion efficiency than GaAs. However, the papers are silent to mention that DAST is expensive, is an extremely difficult material to handle, is hygroscopic, hence rapidly ages and so is virtually useless for commercial use. Another approach, which has received a lot of attention in the literature,¹⁹ is the idea of using a magnetic field to increase the conversion efficiency of a THz emitter. However this technique requires cumbersome and expensive 4 Kelvin superconducting magnets.

What is needed is a potentially low-cost approach based on a relatively mature semiconductor technology that is capable of operating at room temperature. Hence we propose utilising wide-gap semiconductors. GaN represents the most mature and best candidate in terms of the required electrical characteristics as shown in Table 1.

Table 1: Comparison of the major characteristics of GaAs and GaN.

Characteristic	Material	
	GaAs	GaN
Crystal structure	zincblende	wurzite
Lattice constant (Å)	5.65	4.51
Energy gap (eV)	1.42	3.4
Melting point (°C)	1238	1500
Thermal conductivity at 300 K ($\text{Wcm}^{-1}\text{K}^{-1}$)	0.46	1.3
Breakdown field (kV/cm)	400	2000
Effective electron mass	$0.067m_e$	$0.2m_e$
Effective hole mass	$0.50m_e$	$0.80m_e$
Refractive index	3.3	2.33
Electron mobility at 300 K (cm^2/Vs)	8500	500
Saturation velocity (cm/sec)	0.6×10^7	2×10^7

The significance of moving from GaAs to GaN based photoconductive antenna emitters, is that electrode bias can be increased by about a factor of 8. As output power is proportional to the square of the bias, higher power THz beams will be achievable thus opening up a wider range of biomedical applications. Current T-Ray systems are severely restricted by their low output power, with dermal tissue penetration depths limited to approximately 3 mm.¹⁰

Wide bandgap semiconductors such as III-V nitrides present a high critical field (2 MV/cm for GaN and 0.4 MV/cm for GaAs), high carrier saturation velocity (2×10^7 cm/sec for GaN and 0.6×10^7 cm/sec for GaAs) and good thermal conductivity ($1.3 \text{ Wcm}^{-1}\text{K}^{-1}$ for GaN and $0.46 \text{ Wcm}^{-1}\text{K}^{-1}$ for GaAs). By controlling the material growth conditions one can tailor the carrier lifetime for particular applications. For example, THz generation requires short carrier lifetime in order to permit fast recombination and generation of pulses with fast switching characteristics. Moreover, the use of GaN-based material for photoconductive switches is expected to allow generation of higher power level T-rays than currently possible using traditional III-V semiconductors such as GaAs.

III-V nitride samples can be grown using a MOCVD system, using H_2 carrier gas, and trimethylgallium (TMGa), trimethylaluminium (TMAI) and ammonia (NH_3) as Ga, Al and N precursors, respectively. Depending on the particular growth requirements, the system can be operated under low or high-pressure conditions. Both sapphire and SiC substrates can be used for the growth of GaN and section 3.1 considers their suitability in terms of THz transmission properties.

3.1. GaN Substrate Selection

GaN wafers are extremely brittle and until recently have been difficult to reliably fabricate without another supporting substrate. The two most common materials used for this purpose are silicon carbide (SiC) and sapphire (Al_2O_3). There is a great deal of interest in fabricating free-standing GaN substrates fuelled by their wide application in blue-green light emitting diodes (LEDs) and laser diodes (LDs). Recent techniques have succeeded in separating thick layers of GaN from sapphire and SiC substrates using techniques such as hydride vapour phase epitaxy (HVPE).^{20, 21} This paper focusses solely on thin GaN layers on sapphire and SiC substrates, however free-standing GaN substrates are a further promising option worthy of future study.

For efficient conversion from the optical to THz beam, via a photoconductive antenna, the optical femtosecond pulse should be in the wavelength region corresponding to the bandgap of the material. For GaAs

this requires red light, however for GaN, blue femtosecond pulses are required. As blue light is absorbed more highly at shallow depths than red light, it is desirable for the incoming blue optical pulse to be incident on the patterned side of the wafer and not the backside. The resulting THz beam will then have to propagate through the remaining SiC or sapphire layer. For this reason it is important to determine the absorption of terahertz radiation in these materials. To this end samples of SiC and sapphire wafers have been characterised using an all optical T-ray system. Figure 1 shows the reference T-ray pulse of the system. The samples tested were both thin wafers, the sapphire sample was $400\ \mu\text{m}$ thick and the SiC sample thickness was $420\ \mu\text{m}$. The wafers were aligned at normal incidence to the THz field so the results shown are a combination of reflection at the interfaces and absorption within the sample. These results allow us to determine the absorption of the sapphire and SiC samples. Figures 2 and 3 show the responses of sapphire and SiC respectively. Crystalline sapphire has been characterised in the far-infrared previously,²² however this study allows a simple comparison of similar thin samples of sapphire and SiC. It is obvious from these responses that SiC allows much lower transmission at THz frequencies. Using these results the far infrared transmission spectrum for each of the samples can be calculated. This is done by first estimating the power spectral density of the measured pulses (using Welch's algorithm²³) as shown in Figures 4, 5 and 6 and then taking the ratio of the sample and reference spectra. Figures 7 and 8 show the calculated power transmission coefficients. Most of the terahertz energy is at frequencies below 1 THz therefore the transmission coefficients above 1 THz become increasingly noisy. A simple smoothing filter has been applied to the transmission spectra to reduce the noise in the measurements. A box filter was implemented to average each coefficient with its nearest neighbours.

These preliminary measurements indicate that the bulk transmission efficiency for the samples we tested over the frequency range 0.1 to 2 THz are 50.2 % for the sapphire sample and 1.8 % for the SiC sample. Thus sapphire appears the logical substrate choice for future work on GaN terahertz emitters.

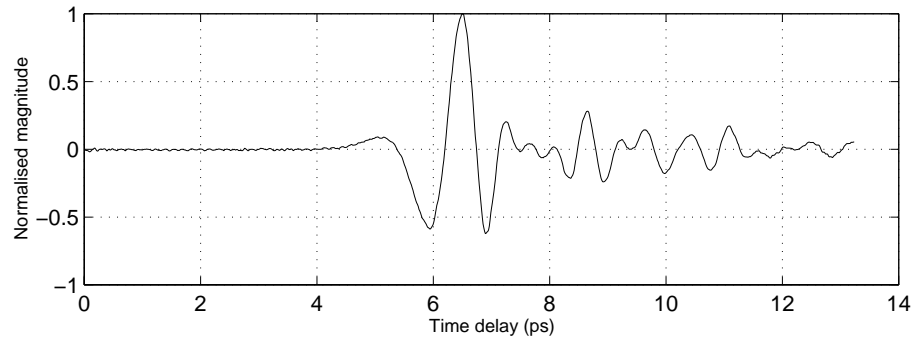


Figure 1. Reference T-ray pulse. This shows the response of the T-ray system with no sample present. The system utilised a 800 nm Ti:sapphire SP Hurricane femtosecond laser with a repetition rate of 997 Hz, pulse width of 150 fs and optical power of 9.6 mW. This light was incident on a $\langle 110 \rangle$ ZnTe emitter to generate the terahertz pulse. The output was measured using a SR830 lock in amplifier with a time constant of 100 ms.

3.2. Evaluation of GaN's Terahertz Response

As discussed in the previous section the properties of the generating optical pulses require that they are incident on the patterned side of the wafer. Thus the terahertz pulses must propagate through the GaN layer as well as the substrate. In this section we consider the terahertz response of a gallium nitride wafer fabricated on a sapphire substrate.

The sapphire substrate was $400\ \mu\text{m}$ thick, with a $1.3\ \mu\text{m}$ layer of GaN. The sample was tested using the same all optical terahertz system described in Section 3.1. Figures 9, 10 and 11 show the time domain response, frequency domain response and transmission spectrum respectively for the GaN on sapphire wafer in the terahertz regime. It can be seen that the sample response is very similar to that of sapphire alone (see Section 3.1) and it can therefore be concluded that the thin film of GaN has very low absorbance over the frequency range of interest.

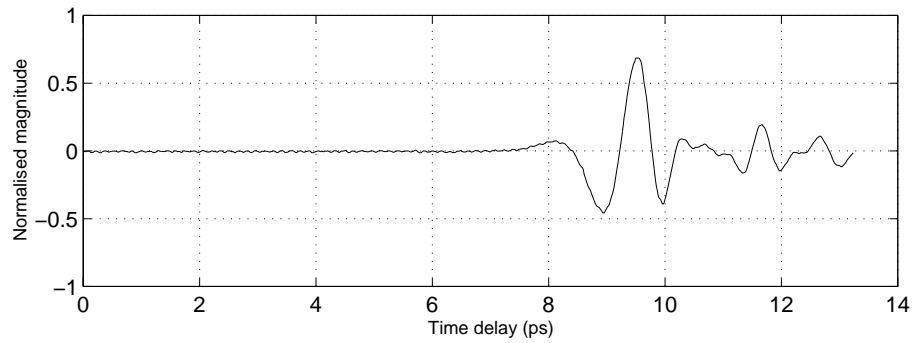


Figure 2. Terahertz pulse after transmission through a sapphire shard of thickness $400\ \mu\text{m}$. This was measured with the same system used for Figure 1. The magnitude of the plot has been normalised to the peak value of the reference pulse, shown in Figure 1.

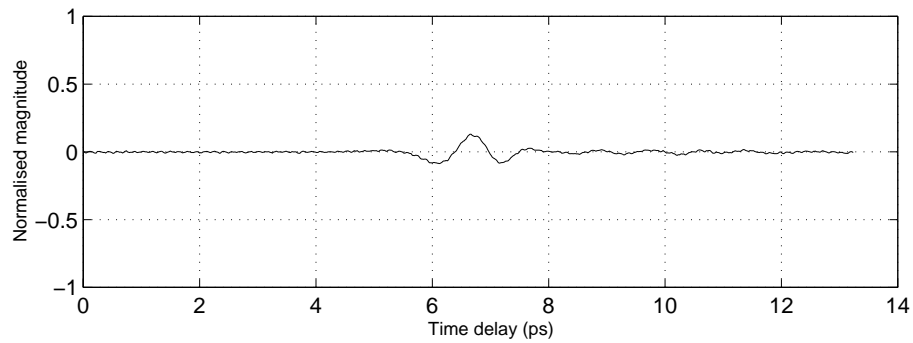


Figure 3. Terahertz pulse after transmission through a SiC (6H-SiC) wafer, bandgap 3eV , $420\ \mu\text{m}$ thick. This was measured with the same system used for Figure 1. The magnitude of the plot has been normalised to the peak value of the reference pulse, shown in Figure 1.

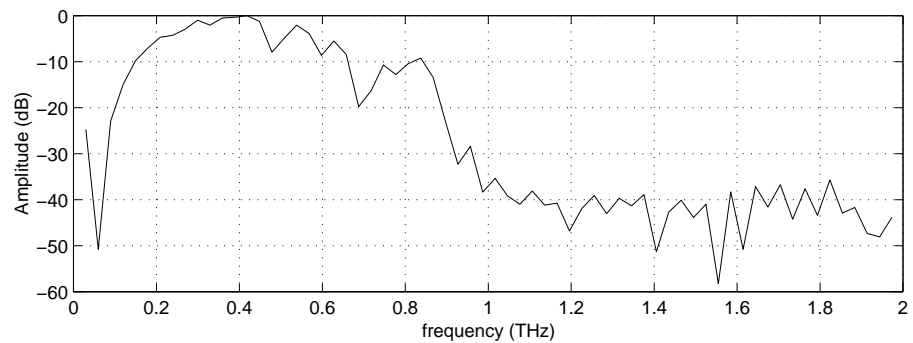


Figure 4. Power spectrum of reference T-ray pulse. This shows the power spectral density of the pulse shown in Figure 1. The PSD is calculated using Welch's algorithm and plotted in decibels.

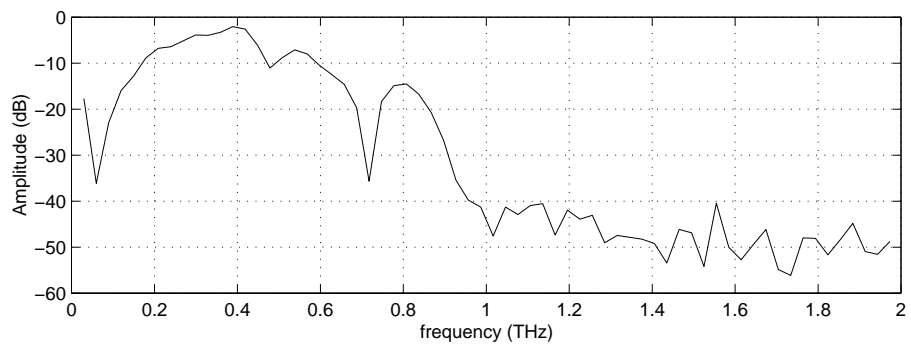


Figure 5. Power spectrum of a sapphire wafer. This shows the power spectral density of the pulse shown in Figure 2. The PSD is calculated using Welch's algorithm and plotted in decibels.

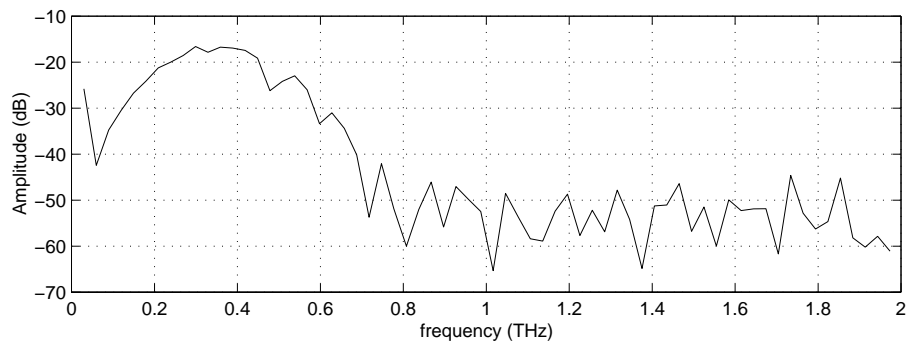


Figure 6. Power spectrum of a silicon carbide wafer. This shows the power spectral density of the pulse shown in Figure 3. The PSD is calculated using Welch's algorithm and plotted in decibels.

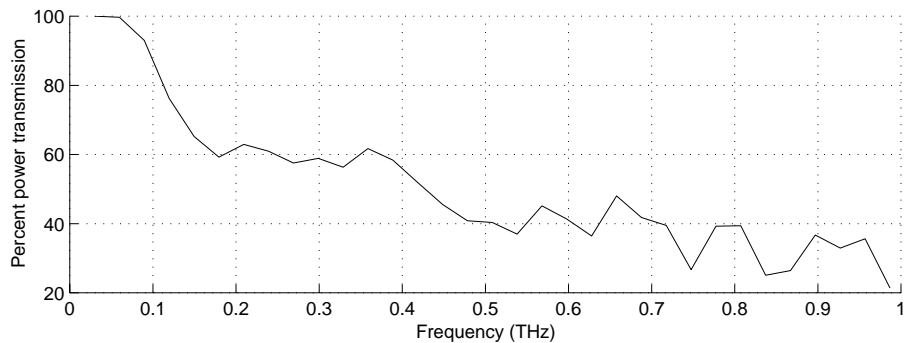


Figure 7. Far-infrared transmission spectrum of the sapphire wafer. The spectrum is calculated by dividing the power spectrum of the sapphire sample by the spectrum of the reference response. The data has been smoothed as described in the text.

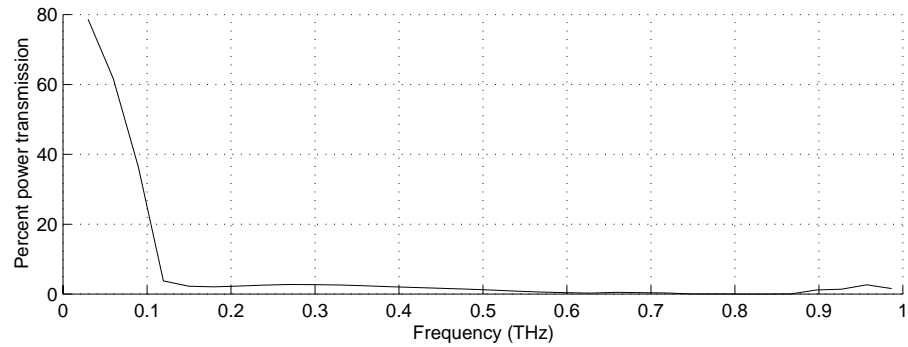


Figure 8. Far-infrared transmission spectrum of the silicon carbide wafer. The spectrum is calculated by dividing the power spectrum of the SiC sample by the spectrum of the reference response. The data has been smoothed as described in the text.

From these measurements the bulk transmission efficiency for the GaN on sapphire sample over the frequency range 0.1 to 2 THz was calculated to be 51.8 %. This is comparable to similar samples of GaAs (approximately 50 % for a GaAs wafer 600 μm thick)²⁴ and is an extremely promising result. The attenuation of the terahertz emitter material is of particular importance if novel reflection geometries are to be realised as the emitter material is positioned in the return path of the reflected terahertz beam.²⁴

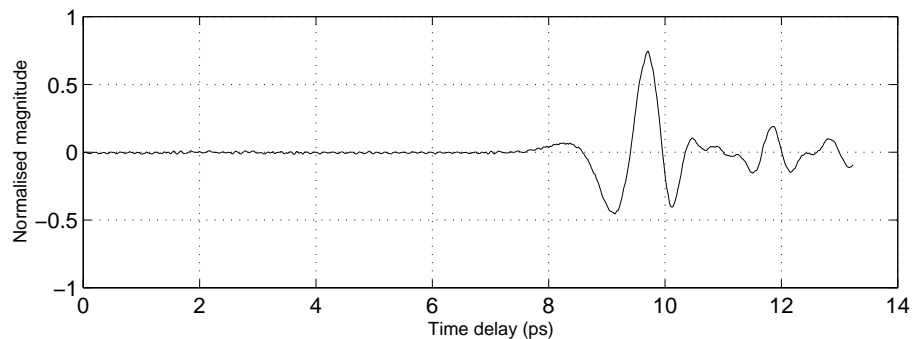


Figure 9. Terahertz pulse after transmission through a thin layer of hexagonal GaN (1.3 μm thick) on a c-plane sapphire substrate of thickness 400 μm . This was measured with the same system used for Figure 1. The magnitude of the plot has been normalised to the peak value of the reference pulse, shown in Figure 1.

3.3. Future Challenges

A great many questions must be answered before efficient, high power GaN THz emitters can be realised. This section highlights a number of the potential challenges to be overcome and discusses the future directions for this research.

As discussed in Section 3.1, a GaN THz emitter requires blue femtosecond pulses of light. For PDAs fabricated on GaAs red pulses are easily obtainable from commercial Ti:Sapphire lasers. However, unfortunately there is no known naturally blue femtosecond laser. Leading edge solid-state Ti:Sapphire lasers are in the red regime, not blue. This problem may be overcome through the use of a Ti:Sapphire laser in conjunction with a frequency doubling method, to produce the required blue light. Frequency doubling has been successfully reported^{25,26} via second harmonic generation (SHG) by having the red pulses incident on a potassium niobate crystal. Improved results are provided with a barium borate crystal where blue pulses as short as 16 fs have been reported.²⁷ It is not clear whether the poorer performance of potassium niobate was due to intrinsic

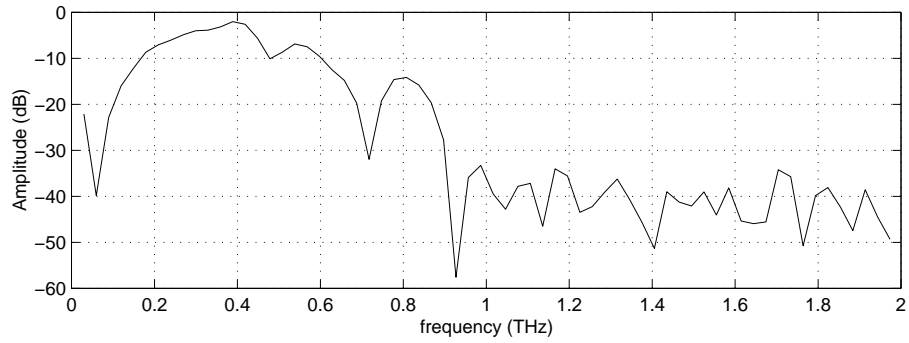


Figure 10. Terahertz power spectrum of GaN on a sapphire substrate. This shows the power spectral density of the pulse shown in Figure 9. The PSD is calculated using Welch's algorithm and plotted in decibels.

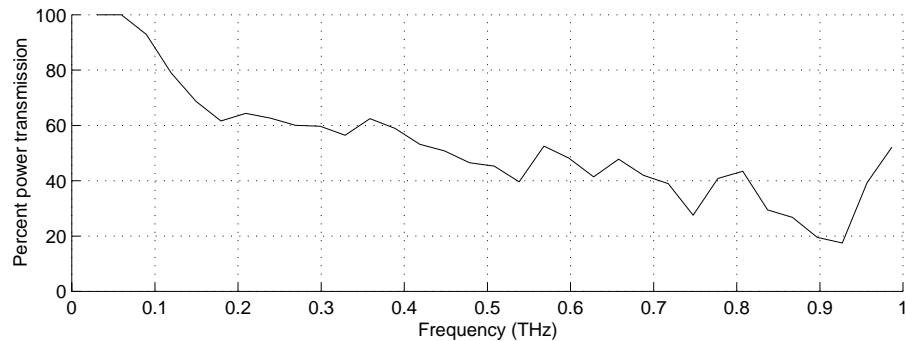


Figure 11. Far-infrared transmission spectrum of GaN on a sapphire substrate. The spectrum is calculated by dividing the power spectrum of GaN on sapphire by the spectrum of the reference response. The data has been smoothed as described in the text.

material dispersion or, in fact, due to the crystal thickness used and other non-optimal system parameters.^{25, 26} Due to the conversion efficiency of SHG, up to a 50 % loss in optical power may be experienced, however this will be more than compensated by the square law dependence of THz power on the photoconductive antenna bias with the use of GaN.

Another challenge with the use of femtosecond pulses is that, due to their short durations, the peak powers can be extremely high, causing THz beam power to drop off due to higher order non-linearities. For this reason a careful trade-off analysis of GaN antenna performance, as a function of optical average power and pulse width must be performed.

A further open question is the optimal geometry of the GaN antenna. The options range from simple parallel electrode antennas with spacings varying between 5 microns and 5 mm (say) to more complicated interdigitated geometries. One potential problem with the interdigitated structures is that neighbouring fingers may induce opposing dipoles leading to cancellation. This may be overcome via patterning an opaque layer over alternate electrode gaps. Another important question is the optimisation of the GaN fabrication process itself. Detrimental effects such as *photoconductivity persistence* in GaN can be controlled via an appropriate vertical growth regime.

Another important goal of this research is to model the photogeneration and photocollection process in the GaN-based substrate to determine the optimum active layer thickness for efficient photogeneration, to maintain good conversion efficiency. As blue light tends to be absorbed at shallow depths, this will favourably mean that thick GaN layers will not be necessary.

Injector barrier designs are another open area of research and may result in faster carrier dynamics. These consist of AlGa_N and InGa_N material. n⁺-Ga_N layers on AlGa_N may contain defects and dislocations. This does not, however, impact device performance as it is in a non-critical region used only for contacting the carrier launcher. The AlGa_N injectors require growth material that is either employed with its residual carrier density (usually in the range of 10¹⁷-10¹⁸ cm⁻³ in the case of AlGa_N) or with small intentional doping values (up to about mid-10¹⁸ cm⁻³) depending on design. No significant impact is therefore envisaged in terms of limitations imposed in doping Al-rich (ie. greater than 25% Al) AlGa_N. The control of the Al-mole fraction allows adjustment of barrier height as necessary for controlling the carrier energy. The Al composition is thought to determine the value of the resulting electric field due to piezoelectric related effects and can thus have a crucial role on determining the carrier dynamics to be studied. The impact of AlGa_N composition and thickness on the transport properties is of great importance to this research and remains an open question.

Compositional grading of AlGa_N requires the determination of the dependence of the Al content in AlGa_N on the TMAI/TMGa ratio in the gas phase, as well as growth rates for different compositions in order to allow exact grading profiles with the desired thickness.

Optimisation of InGa_N is also necessary since the growth of this material is known to lead to phase-separation due to thermodynamical and chemical mismatch and instabilities between Ga_N and In_N. Since these layers are designed to be rather thin, one expects their crystalline properties to be good near the InGa_N/Ga_N interface, but also in a major part of the injector. However, it is known that as the InGa_N layer thickness increases, the crystal quality deteriorates and the In mole fraction increases.

It is important to determine the minimum thickness necessary to obtain the required barrier height and current injection as related to good crystalline quality and desired In mole fraction. A further crucial question in assessing the benefits of Ga_N terahertz emitters is to evaluate the maximum bias that can be applied across Ga_N electrodes, and to characterise the generated T-ray power as a function of bias.

4. CONCLUSION

We have introduced the concept of a novel terahertz emitter, namely a photoconductive antenna on gallium nitride. Ga_N features a number of advantages over the popular GaAs technology. Furthermore it has a much greater semiconductor breakdown voltage allowing a significant increase in terahertz output power. The far-infrared absorption of two potential substrates for a Ga_N emitter, sapphire and SiC have been measured and sapphire was found to be much more suitable for this application. A Ga_N wafer on a sapphire substrate was characterised using an all optical terahertz system and the absorption of Ga_N was found to be negligible compared to that of the substrate.

Many open questions remain in this field. In particular further research is required in optimising the generation of efficient femtosecond sources matched to the bandgap of Ga_N and in the investigation of novel antenna geometries. Injector barrier designs for faster carrier dynamics and optimisation of the fabrication process and layer thicknesses are other potentially fruitful research directions.

ACKNOWLEDGMENTS

This work was funded by the Australian Research Council (ARC). Thanks are due to Prof. X.-C. Zhang's group at Rensselaer Polytechnic Institute (RPI) for their assistance with the measurements.

REFERENCES

1. Y.-R. Shen, "Far-infrared generation by optical mixing," *Progress in Quantum Electronics* **4**(3), pp. 207–232, 1976.
2. J. Morris and Y. R. Shen, "Far-infrared generation by picosecond pulses in electro-optic materials," *Optics Communications* **3**(2), pp. 81–84, 1971.
3. K. H. Yang, P. L. Richards, and Y. R. Shen, "Generation of far-infrared radiation by picosecond light pulses in LiNbO₃," *Applied Physics Letters* **19**(9), pp. 320–323, 1971.

4. D. H. Auston and P. R. Smith, "Generation and detection of millimeter waves by picosecond photoconductivity," *Applied Physics Letters* **43**(7), pp. 631–633, 1983.
5. D. M. Mittleman, R. H. Jacobson, and M. C. Nuss, "T-ray imaging," *IEEE Journal of Selected Topics in Quantum Electronics* **2**(3), pp. 679–692, 1996.
6. M. C. Nuss, "Chemistry is right for T-rays," *IEEE Circuits and Devices* **12**(2), pp. 25–30, 1996.
7. D. M. Mittleman, M. Gupta, R. Neelamani, R. G. Baraniuk, J. V. Rudd, and M. Koch, "Recent advances in terahertz imaging," *Applied Physics B: Lasers and Optics* **68**(6), pp. 1085–1094, 1999.
8. R. M. Woodward, B. Cole, V. P. Wallace, D. D. Arnone, R. Pye, E. H. Linfield, M. Pepper, and A. G. Davies, "Terahertz pulse imaging of in-vitro basal cell carcinoma samples," in *Conference on Lasers and Electro-Optics 2001*, pp. 329–330, SPIE, 2001.
9. B. Ferguson and D. Abbott, "Signal processing for T-ray bio-sensor systems," in *Smart Electronics and MEMS II*, **4236**, pp. 157–169, SPIE, (Melbourne, Australia), 2001.
10. D. D. Arnone, C. M. Ciesla, A. Corchia, S. Egusa, M. Pepper, J. M. Chamberlain, C. Bezant, E. H. Linfield, R. Clothier, and N. Khammo, "Applications of terahertz (THz) technology to medical imaging," in *Terahertz Spectroscopy and Applications*, **3828**, pp. 209–219, SPIE, (Munich, Germany), 1999.
11. A. G. Markelz, A. Roitberg, and E. J. Heilweil, "Pulsed terahertz spectroscopy of DNA, bovine serum albumin and collagen between 0.1 and 2.0 THz," *Chemical Physics Letters* **320**(1-2), pp. 42–48, 2000.
12. D. Arnone, C. Ciesla, and M. Pepper, "Terahertz imaging comes into view," *Physics World* (4), pp. 35–40, 2000.
13. E. Budiarto, "Study of non-linear electrodynamics in high-Tc superconductors by use of intense terahertz pulses," in *Proc. Conf. on QELS*, **12**, pp. 41–42, (Baltimore), 1997.
14. B. E. Cole, J. B. Williams, B. T. King, M. S. Sherwin, and C. R. Stanley, "Coherent manipulation of semiconductor quantum bits with terahertz radiation," *Nature* **410**, pp. 60–65, 2001.
15. G. A. Mourou, C. V. Stancampiano, and D. Blumenthal, "Picosecond microwave pulse generation," *Applied Physics Letters* **38**(6), pp. 470–472, 1981.
16. G. A. Mourou, C. V. Stancampiano, A. Antonetti, and A. Orszag, "Picosecond microwave pulses generated with a subpicosecond laser driven semiconductor switch," *Applied Physics Letters* **39**(4), pp. 295–296, 1981.
17. D. You, R. R. Jones, R. H. Bucksbaum, and D. R. Dykaar, "Generation of high-power sub-single-cycle 500-fs electromagnetic pulses," *Optics Letters* **18**(4), pp. 290–292, 1993.
18. K. K. et al, "Difference-frequency terahertz-wave generation from 4-dimethylamino-*n*-methyl-4-stilbazolium-tosylate by use of an electrically tuned Ti:sapphire laser," *Optics Letters* **24**(15), pp. 1065–1067, 1999.
19. R. McLaughlin, Q. Chen, A. Corchia, C. M. Ciesla, D. D. Arnone, X. Zhang, G. A. C. Jones, E. H. Linfield, and M. Pepper, "Enhanced coherent terahertz emission from indium arsenide," *Journal of Modern Optics* **47**(11), pp. 1847–1856, 2000.
20. Y. V. Melnik, K. V. Vassilevski, I. P. Nikitina, A. I. Babanin, V. Y. Davydov, and V. A. Dmitriev, "Physical properties of bulk GaN crystals grown by HVPE," *MRS Internet J. Nitride Semicond. Res* **2**(39), 1997.
21. H. M. Kim, J. E. Oh, and T. W. Kang, "Preparation of large area free-standing GaN substrates by HVPE using mechanical polishing liftoff method," *Materials Letters* **47**(4), pp. 276–280, 2001.
22. D. Grischkowsky, S. Keiding, M. van Exter, and C. Fattinger, "Far-infrared time-domain spectroscopy with terahertz beams of dielectrics and semiconductors," *Journal of the Optical Society of America B: Optical Physics* **7**(10), pp. 2006–2015, 1990.
23. J. G. Proakis and D. G. Manolakis, eds., *Digital Signal Processing - Principles, Algorithms, and Applications*, Prentice-Hall, London, 3rd ed., 1996.
24. S. Mickan, X. C. Zhang, J. Munch, and D. Abbott, "Chemical sensing in the submillimeter wave regime," in *Smart Structures and Devices II*, **4235**, pp. 434–442, SPIE, (Melbourne, Australia), 2001.
25. A. M. Weiner, A. M. Kan'an, and D. E. Leaird, "High efficiency blue generation by frequency doubling of femtosecond pulses in a thick nonlinear crystal," *Optics Letters* **23**(18), pp. 1441–1443, 1998.
26. D. Gunzun, Y. Li, and M. Xiao, "Blue light generation in single-pass frequency doubling of femtosecond pulses in KNbO₃," *Optics Communications* **180**, pp. 367–371, 2000.
27. D. Steinbach, W. Hugel, and M. Wegener, "Generation and detection of blue 10.0 fs pulses," *Journal of the Optical Society of America B* **15**(3), pp. 1231–1234, 1998.